

AIR QUALITY MODELING: EFFECT OF LAND USE DATABASE USING REMOTE SENSING DATA

Chang-You Tsai¹, Tu-Fu Chen², Yi-Pin Lin³, and Ken-Hui Chang^{4*}

ABSTRACT

In addition to meteorological inputs, land use and emission factor database are also required for simulation of the Biogenic Emission Inventory System (BEIS). The resolution of land use database in the Taiwan BEIS (TBEIS) can be up to 1 km² and this database consists of vegetation species and their spatial distribution in Taiwan with a total land area of approx 36000 km². The previous Taiwanese land use database was established in 1995, but since then Taiwan has gone through cultural, ecological and seismic changes for more than a decade. As a result, the area and distribution of current land use types needed revision. To complete this revision accurately, recent satellite remote sensing data were used in this research.

In the updated land use database, the new forested area had increased by 2400 km², grass land had increased by 1790 km², paddy fields had increased by 2,100 km² and dry agriculture land had decreased by 1830 km². There was a net increase of 4460 km² in vegetation area, which equates to about 16% of the total vegetation land area of Taiwan. Simulation of the TBEIS-2 rendered to an increase of 28,000 ton/yr in total BVOCs (6.6%), in which other VOCs (OVOC) increased by 17,000 ton/yr (12.1%) and isoprene increased by 10,000 ton/yr (7.9%). The biogenic emissions obtained by the use of TBEIS-2 with the new land use database are utilized to simulate air quality by the Taiwan Air Quality Monitoring (TAQM). Results indicated that concentrations of ozone and other photochemical pollutants raised in some areas of Taiwan. In the simulation conducted in May 2003, the greatest ozone concentration difference occurred in southern Taiwan and central Taiwan with an increase of 3 ~ 7 ppb in these districts.

Keywords: Model, biogenic emission, land use type, ozone concentration.

1. INTRODUCTION

Ozone is mainly produced by photochemical reactions among volatile organic compounds (VOCs) and NOx in the atmosphere. As a result, these two precursors have to be controlled for reducing O₃ formation. Emission sources of VOCs consist of anthropogenic VOCs and biogenic VOCs (BVOCs). Unfortunately, the BVOC emissions account for a major fraction of total VOCs emitted. For example, over 90% of global annual VOCs are emitted by plants (Guenther *et al.* 1993; Guenther *et al.* 1995). Since forest lands account for 59% of the total area in Taiwan (<http://www.forest.gov.tw>) and previous studies have indicated that BVOCs contribute to about 20% total VOC emissions in Taiwan (Chang *et al.* 2005). The impact of BVOC emissions on ozone pollution in Taiwan is significant, especially during certain seasons and in certain regions that VOC is the controlling factor in O₃ formation (Chen *et al.* 2019; Chang 2008; Chen and Chang 2006).

Manuscript received December 16, 2019; revised February 28, 2020; accepted February 29, 2020.

¹ Ph.D. Student, Dept. of Safety, Health and Environment Engineering, National Yunlin University of Science and Technology, Taiwan 64002, R.O.C

² Assistant Researcher, Dept. of Safety, Health and Environment Engineering, National Yunlin University of Science and Technology, Taiwan 64002, R.O.C.

³ Ph.D. Student, Graduate School of Engineering Science and Technology, National Yunlin University of Science and Technology, Taiwan 64002, R.O.C.

^{4*}Distinguished Professor, (corresponding author), Dept. of Safety, Health and Environment Engineering, National Yunlin University of Science and Technology, Taiwan 64002, R.O.C. (e-mail: changken@yuntech.edu.tw).

To estimate BVOC emissions more accurately, land use types must be classified and updated. Currently, the database of land use-types is based on a survey data of forest resources and land use in Taiwan conducted by the Forestry Bureau in 1995. As 20 years have already elapsed since this study was completed, land use pattern has been dramatically changed due to typhoons, mudslides and more importantly, a high magnitude earthquake on September 21, 1999. Also, both cultural and ecological changes such as urban development and highway construction also has a considerable effect on land use. Consequently, the need for developing a new land use database is urgent.

To modify the changes and variations in land use types, the satellite remote sensing data of vegetation areas in Taiwan collected by the Center for Space and Remote Sensing Research of National Central University (CSRSR) from 2005 to 2006 were adopted in this study. The use of remote sensing for classifying land use patterns is not novel and has also been widely used to determine non-point sources of pollution (e.g., Chen *et al.* 2018; Prakash Basnyat *et al.* 2000), management of agricultural watershed (Pandey *et al.* 2009), rural land use changes (Cheng *et al.* 2015; Peng *et al.*, 2008; Chen *et al.* 2006), erosion management (Kheir *et al.* 2008), and dry deposit modeling (Feldman *et al.* 2007). However, the application of land use patterns developed from remote sensing for BVOC modeling is rather scarce (Wiedinmyer *et al.* 2001; Wang *et al.* 2003; Liu *et al.* 2019). Further, to the authors' best knowledge, the use of remote sensing to correcting land use types to first estimate BVOC quantity and subsequently using the estimated BVOC amount for predicting diurnal O₃ concentration have not been performed before.

Consequently, this study was undertaken to use remote sensing to correct land use patterns, in particular changes of major vegetation species, vegetation areas and their spatial distribution. Two

databases (old and new) were respectively used to estimate BVOCs. Finally, to examine the difference in O₃ concentration between the two estimated BVOCs datasets, an O₃ model was used in conjunction with them to predict diurnal O₃ concentrations.

2. MATERIALS AND METHODS

2.1 Satellite Remote Sensing Data

This remote sensing data in Taiwan from 2005 to 2006 collected by CSRSR were used. An example of which is shown in Fig. 1. These image data were sorted from remote sensing image pictures obtained by FORMOSAT-2 around the island. The size of images in the data set is 26000 × 47500 pixels, with the highest spatial resolution being 8 × 8 m² with an image identification ratio of 79%. Except for unidentified data, twelve types of objects shown in Figure 1 can be identified; they are: (1) clouds, (2) water bodies, (3) buildings, (4) seas, (5) roads, (6) riverbeds, (7) beaches, (8) dry agriculture lands, (9) grass lands, (10) paddy fields, (11) small amount of plants, and (12) plants in the mountains.

2.2 Correction and Updating Land use Database

The process of updating the land use database is illustrated in Fig. 2. First, the types, areas and grid coordinates from the original land use database were determined. Incidentally, although the maximum resolution for the original land use database was 1 × 1 km², each grid may have covered up 83 land use types, including 68 vegetation and 15 non-vegetation types. The newly

acquired remote sensing data were first classified into vegetation and non-vegetation types. If the object was a non-vegetation type (e.g., water bodies, buildings, seas, roads, riverbeds, beaches), the comparison between the original land use database and the newly acquired data was omitted. Conversely, if the remote sensing data revealed vegetation types, then a comparison with the original land use database was made. Specifically, if they showed a common vegetation type (paddy fields, dry agriculture lands and grass lands), the satellite area data were directly entered into the new land use database. If the result of a comparison indicated different vegetation types, further judgment on the same vegetation species found in that grid was made as follows. The proportional distribution of vegetation type would be ascertained if the vegetation area of satellite data is different from the original vegetation area in the same grid. If satellite data indicated the vegetation area in the grid of original non-vegetation area, it would be marked as a new vegetation type. Because satellite data could not distinguish the detailed vegetation types as in the original land use database, new vegetation types would be classified into two types of forests, according to their altitude (higher or lower than 1,500 m). Essentially, broadleaved forests would be assigned for the new vegetation type with lower altitude (< 1,500 m), while coniferous forests would be assigned for the one with higher altitude (> 1,500 m).

For non-vegetation types, and the remaining four vegetation items (paddy fields, dry agriculture lands and grass lands, proportional distribution) and new vegetation types of broadleaved and coniferous forests were integrated and entered into the grids of land use type and area for completion of a new land use database.

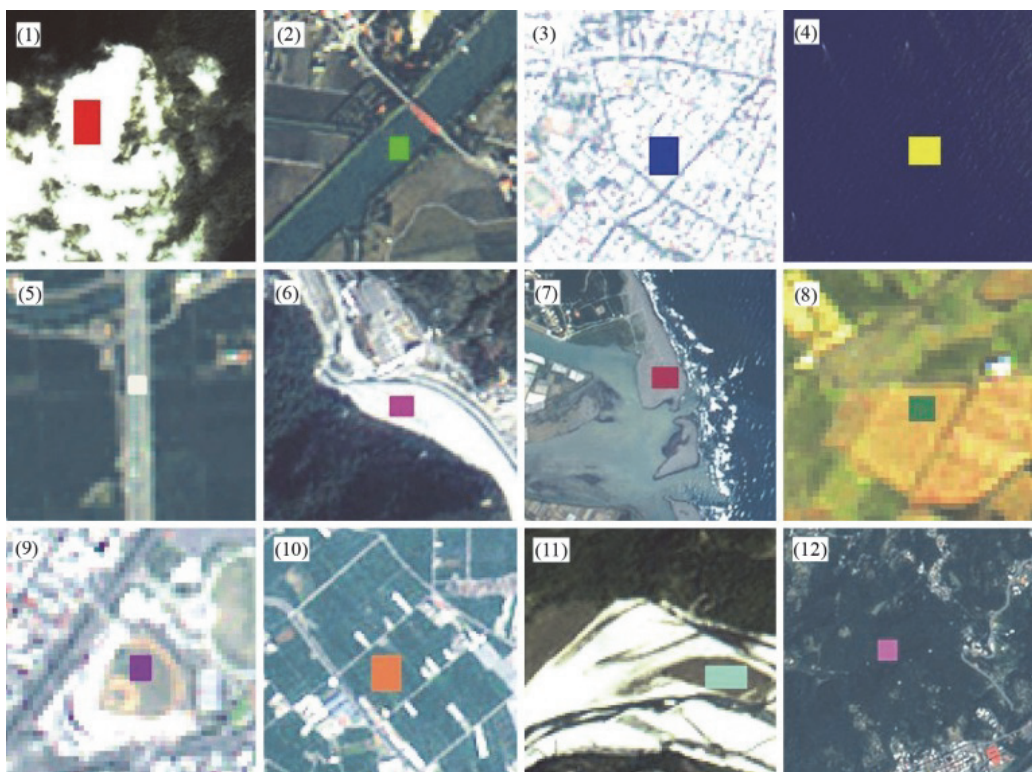


Fig. 1 Types of Remote Sensing Data and Classification Method. (1) clouds, (2) water bodies, (3) buildings, (4) seas, (5) roads, (6) riverbeds, (7) beaches, (8) dry agriculture lands, (9) grass lands, (10) paddy fields, (11) small amount of plants, and (12) plants in the mountains. (Small squares in the photo is the selected standard photo image for species judgment)

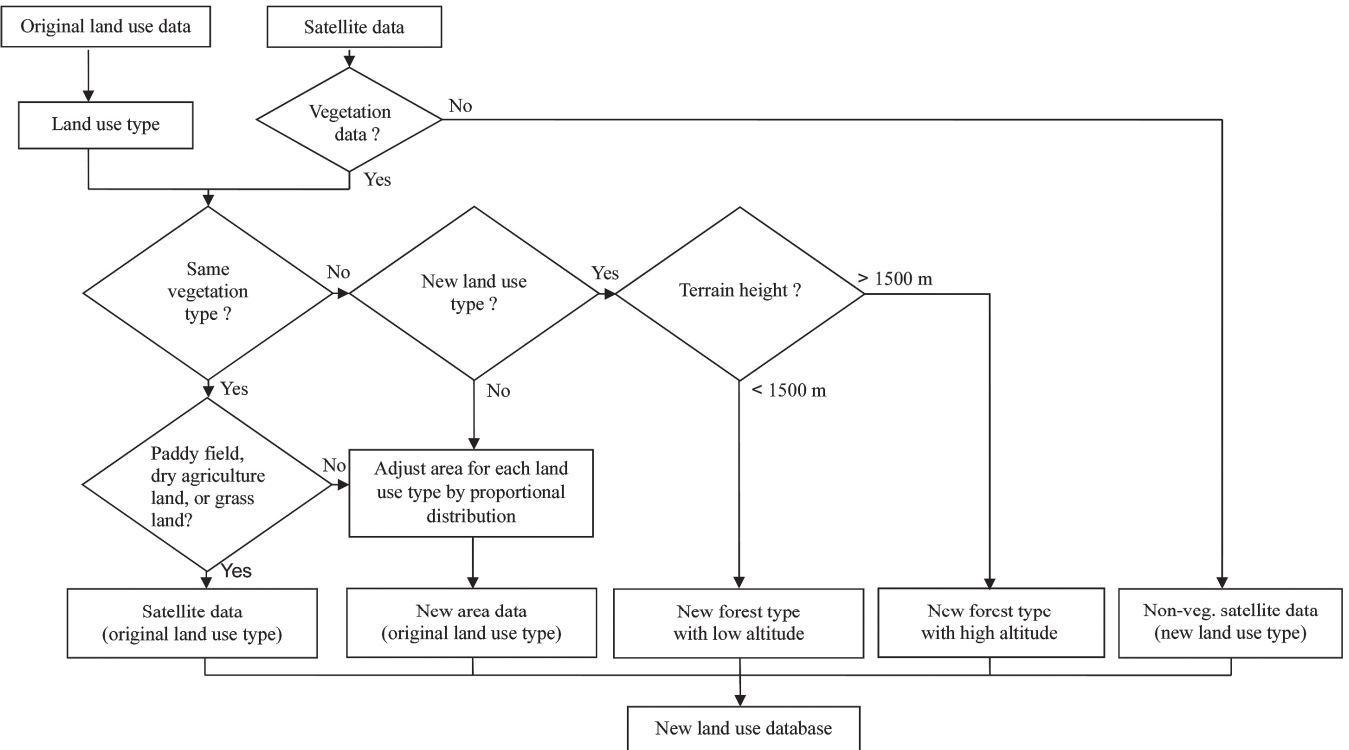


Fig. 2 Process of Updating Land use Database of Taiwan

2.3 Taiwan Biogenic Emission Simulation

The biogenic emission model used was from Taiwan Biogenic Emission Inventory System version 2 (TBEIS-2) (Chang *et al.* 2009). The model considers (1) 83 land use types (2) emission fluxes for various vegetations, (3) energy balance module to account for leaf temperature, and (4) correction terms for leaf temperature and photosynthetically active radiation (PAR). The model output includes 4 categories of 33 BOVCs including isoprene, methylbutenol (MBO), 14 species of monoterpenes and 17 other BVOCs.

There are four components contained in the TBEIS-2 model including the land-use pattern, emission factor for vegetations, leaf energy balance model, and PAR flux corrections. The input parameters considered in the model include RH, wind velocity, atmospheric pressure, cloud cover, and precipitation. These parameters with ambient temperature and PAR are required for leaf temperature simulation. The leaf energy balance model used to predict leaf temperature was incorporated into TBEIS-2 to account for the conversion from ambient temperature to leaf temperature by biochemical and biophysical processes.

Because natural emissions of VOCs are very sensitive to changes in land cover (Monks *et al.* 2009), the land use database is crucial to the simulations. The available land use databases used in TBEIS-2 are the land use database of Taiwan Forestry Bureau (Chang 1999, referred as TFBLD) for natural forests and the land use database of Taiwan Emission Data System (CTCI 1999, referred as TEDSLD) for agricultural vegetations. Both data sets have spatial resolutions of 1 km by 1 km. The area coverage of the TFBLD is mostly concentrated on the governmental land around and within mountain regions. In this study, the original land use database for emission model was based on TFBLD

with supplemental information from TEDSLD for areas not covered by TFBLD, especially the dry agriculture land and paddy fields in the plain regions. Consequently, the original land use patterns were classified into 83 land-use types including 48 forests, 16 agricultural-lands, 4 other vegetations, and 15 non-vegetation lands. Although the grid area in TBEIS-2 is 1 km², each grid covers each land use type. Such detailed land use pattern would render better BVOC emission resolution/estimation.

2.4 Air quality Model Simulation

The Taiwan Air Quality Model (TAQM) (Chen and Chang 2006; Chang 2008) was used to simulate O₃ air quality; the impact of updating the land use database was then evaluated. Briefly, the TAQM is a Eulerian grid model incorporating atmospheric transport (horizontal and vertical advection), diffusion, source emission, chemical reactions, cloud effects and dry/wet depositions.

The TAQM is an adaptation and extension of the RADM2 model (Chang *et al.* 1987; Chang 1990), developed for the USEPA. The horizontal coordinate system in the TAQM uses a Lambert conformal projection for the simplicity of numerical execution, whereas TAQM uses a terrain following coordinate system in the vertical direction. The gas phase chemical mechanisms of RADM2 accounting for transformation of 63 species in 158 reactions, developed by Stockwell *et al.* (1990), is adopted in TAQM. The inorganic chemistry reaction includes 14 stable, 4 intermediate and 3 stable species, while the organic chemistry is expressed by 26 stable species and 16 peroxy radicals. Clear sky photolysis rates are simulated as a function of daytime, latitude and height. A series resistance approach is employed to calculate

dry deposition. Concentration changes of trace species due to rainout or chemical reactions of soluble and reactive gases in a cloud are calculated using a box aqueous chemical model. A set of partial differential equations of mass conservation for the atmospheric species is solved numerically with the approximations of finite difference methods. Due to the unique mathematical characteristics, the operator splitting technique is employed to optimize the accuracy of the overall solution and the computational efficiency of the model (Chang *et al.* 2000).

The districts and domains simulated with the TAQM in this study are shown in Fig. 3. Domain-1 includes China, Taiwan, Korea, Japan and Vietnam in East Asia with a grid resolution of $81 \times 81 \text{ km}^2$. Domain-2 consists of southeastern parts of China and Taiwan with a grid resolution of $27 \times 27 \text{ km}^2$. Domain-3 includes the entire area of Taiwan with a resolution of $9 \times 9 \text{ km}^2$. Domain-4 consists of northern, central or southern Taiwan using $3 \times 3 \text{ km}^2$ resolution.

The meteorological information required for simulation is based on MM5 (Fifth-Generation Penn State/NCAR Mesoscale Model) (Grell *et al.* 1993). As the initial and boundary conditions for the grid model significantly affect the simulation results, Domain-1 was simulated first for two days as the initiative simulation of the TAQM to develop the boundary and initial conditions for the subsequent simulations. Domains 1-4 were overlapped and simulated three times to reach the highest grid resolution.

The quantity of Taiwan's anthropogenic VOCs was based on Taiwan Emission Data System (CTCI 1999). As for the an-

thropogenic emissions in East Asia, they were based on the database set developed by Street *et al.* (2003) for NOx and the database established by Frontier Research System for Global Change (hereinafter called FRSGC) (Ohara *et al.* 2007) for non methane hydrocarbons. In addition, these low-resolution anthropogenic emissions incorporated with the population data information of $1 \times 1 \text{ km}^2$ in East Asia to enhance the resolution of emissions for a more elaborate grid model.

3. RESULTS AND DISCUSSION

3.1 Renewal of Land Use Types

The comparison between original and new land use database is shown in Table 1. Clearly, there are significant differences between these two datasets. An additional area of $1,790 \text{ km}^2$ (398% increase) and $2,100 \text{ km}^2$ (65%) was added to grass lands and paddy fields, respectively. Only dry agriculture land was reduced by $1,830 \text{ km}^2$ (61% decrease). A new forest area of $2,400 \text{ km}^2$ was also added with the overall net increase of about $4,460 \text{ km}^2$, which accounts for 16% of the total vegetation area of Taiwan. From the spatial distribution of vegetation differences (Fig. 4), vegetation in the western coastal areas of Taiwan has decreased due to the disappeared coastal windbreak forest; however, vegetation in districts at medium and low elevations around the Central Mountains increases significantly, while vegetation in districts at high elevations decreases in particular.

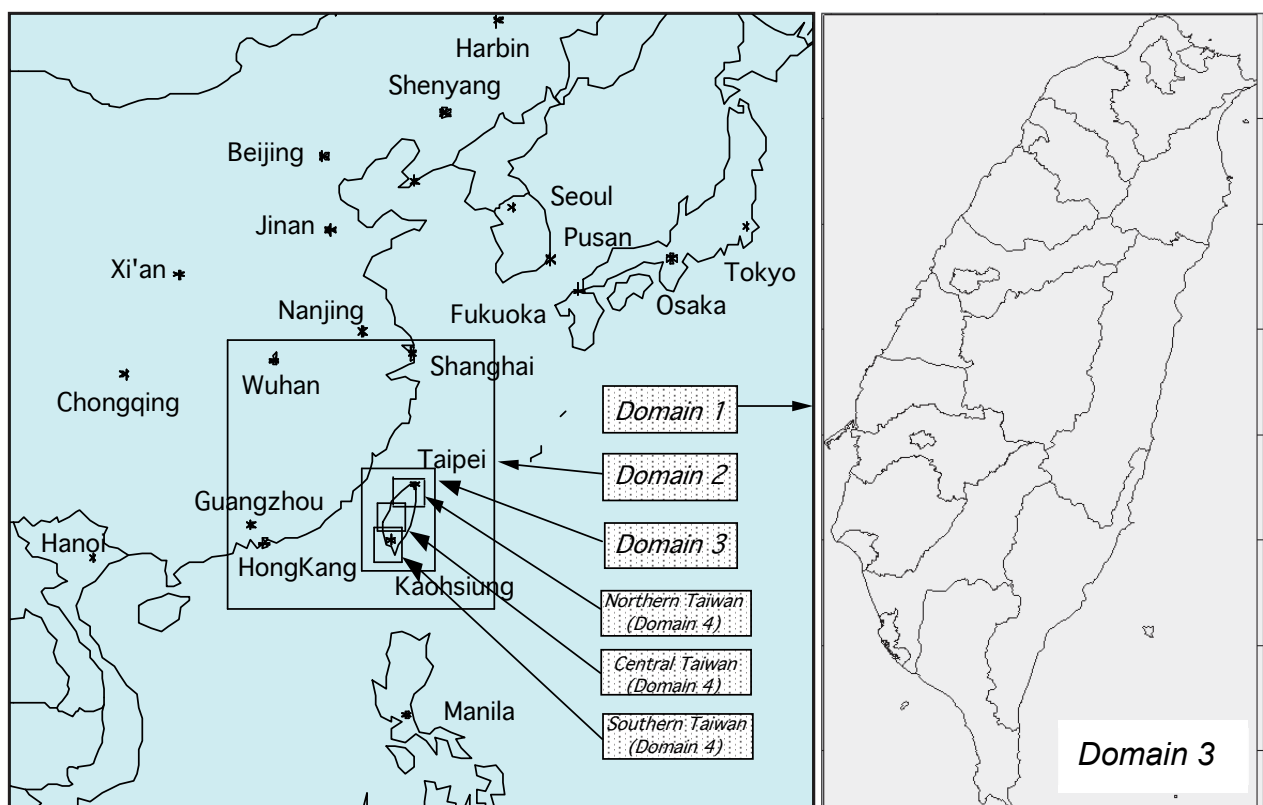
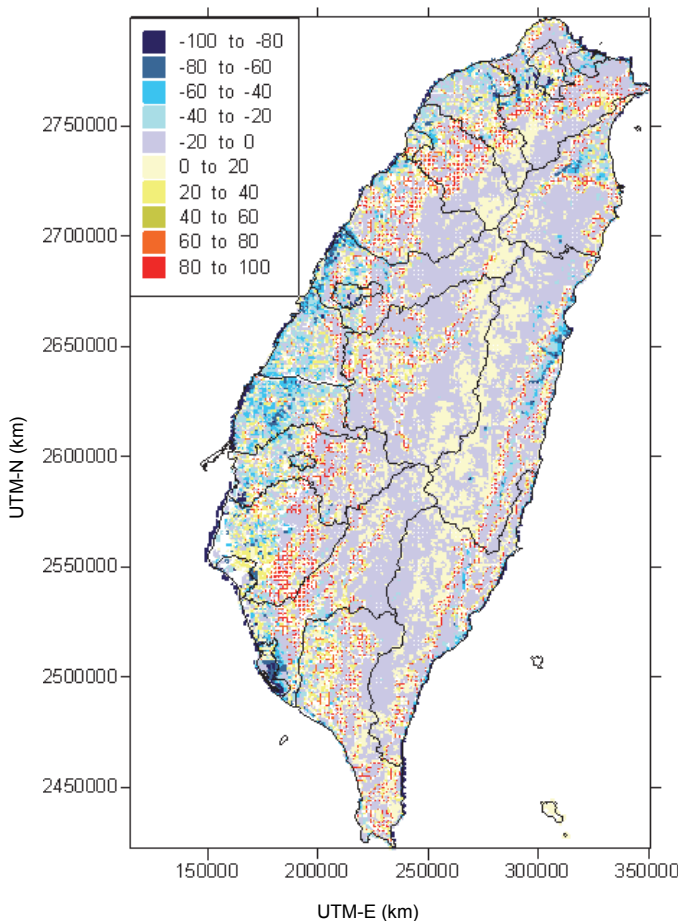


Fig. 3 Configuration of Four Nesting Domains for Simulation in the Study. Domain 3 Covers Whole Taiwan Island

Table 1 Areas of Forests, Grass Land, Paddy Field and Dry Agriculture Land in Original and New Land Use Databases

| Land use type | Original database (km ²) | New database (km ²) | Difference area (km ²) | Difference ratio (%) |
|----------------------|--------------------------------------|---------------------------------|------------------------------------|----------------------|
| Forests | 20580 | 22980 | 2400 | 12 |
| Grass land | 450 | 2240 | 1790 | 398 |
| Paddy field | 3210 | 5310 | 2100 | 65 |
| Dry agriculture land | 2990 | 1160 | -1830 | -61 |
| Total | 27230 | 31690 | 4460 | 16 |

**Fig. 4** Spatial Distribution of Vegetation Difference Ratio (%). (blue: decrease in vegetation; red: increase in vegetation)

3.2 Influence of Land Use Types on BVOC Emissions

The major purpose of updating the land use database is to determine BVOC emissions more accurately to reflect the actual circumstances of Taiwan. The year of 2003 was selected for simulations of BVOC emission using TBEIS-2 and the impact of changes and variations of biogenic emissions in quantity and spatial distribution before and after land use updating was evaluated. Hour-by-hour meteorological data (ambient temperature, wind velocity, relative humidity, atmospheric pressure, fraction of cloud coverage, light and PAR) in each grid interpolated by the data collected from 185 weather stations (25 ground weather stations of the Weather Bureau + 88 synoptic stations + 72 air quality monitoring stations of the EPA) for the whole year of 2003, were used in this study for BVOC simulations.

The differences of total BVOC emissions before and after updating the land use database are listed in Table 2. The isoprene emission increased by 8% for the whole year; which does not appear to be a great amount, but the O₃ formation potential for isoprene is significant. The total BVOC emissions increased to 6.6%, apparently due to an increase in vegetation area of Taiwan by about 16%. In addition to a comparison of the total emissions, the third quarter (July-September), the highest BVOC emission season, of 2003 was selected to examine differences of spatial BVOC distribution. The biogenic emissions increased significantly in the regions at medium and low elevations and decreased slightly in the Central Mountains (Fig. 5). This is consistent with the result of distribution of forest stands shown in Fig. 4. There used to be forest types with lower emission factors in these areas in the previous land use database. After updating the database with satellite remote sensing data, forest stands with higher emission factors were added, which can be seen to cause an obvious increase in emissions. Figure 5 shows these differences in spatial distribution.

Table 2 Comparison of Various BVOC Emissions of Taiwan before and after Updating Land use Database (10³ ton/yr)

| | Isoprene | MBO | Monoterpenes | Other VOCs | Total amount |
|----------------------------|----------|-----|--------------|------------|--------------|
| Original land use database | 127 | 3 | 156 | 141 | 427 |
| New land use database | 137 | 3 | 157 | 158 | 455 |
| Difference | 10 | 0 | 1 | 17 | 28 |
| Difference ratio (%) | 7.9 | 0.0 | 0.6 | 12.1 | 6.6 |

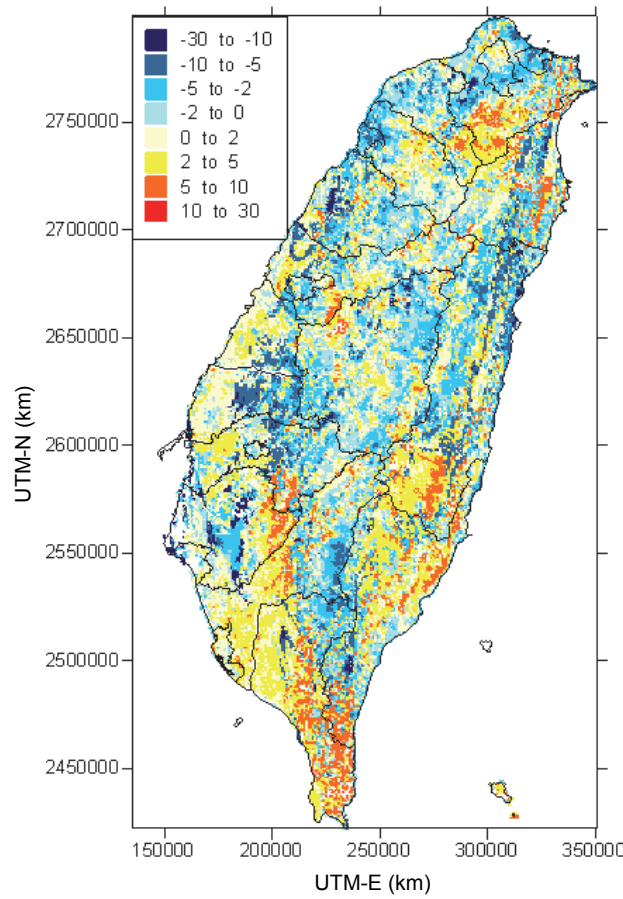


Fig. 5 Spatial Distribution of Total BVOC Emission Differences before and after Updating Land use Database (July-September, 2003). (blue: emissions reduced after updating; red: emissions increased after updating; Unit: ton)

3.3 Influence of Updating Land Use Types on Ozone Spatial Distribution

The selection of simulation episodes was mainly based unique O₃ event. The period between May 20 and 30, 2003 was selected for O₃ simulation analysis due to the presence of high O₃ pollution events. The daily maximum O₃ concentration usually occurs around 14 pm in sub-urban areas. 14:00 on May 25, 2003 was selected to present the influence of the updated land use database of Taiwan. The spatial distribution of difference of simulated O₃ concentrations before and after updating land use database is shown in Fig. 6 at 14:00 on May 25, 2003. It is found that ozone increased significantly in the mountain areas of central and southern Taiwan with the greatest difference of 6 ppb found in the mountain districts of southern Taiwan in particular. The reason for this finding was that the wind in southern Taiwan at this time blew inland and carried ozone to the mountain areas. This is a consistent result when compared to areas that saw an increase in biogenic emissions around the areas at low and medium altitudes.

To discover the greatest difference in ozone before and after the update, the maximum ozone values during the simulation period were entered into each grid and the difference was cal-

culated (Fig. 7). A comparison of the greatest difference in maximum ozone concentrations during the simulation period revealed a significant increase in ozone was also located in the mountain areas of central and southern Taiwan. The greatest increase in ozone was 5-7 ppb in southern Taiwan and 3-6 ppb in central Taiwan.

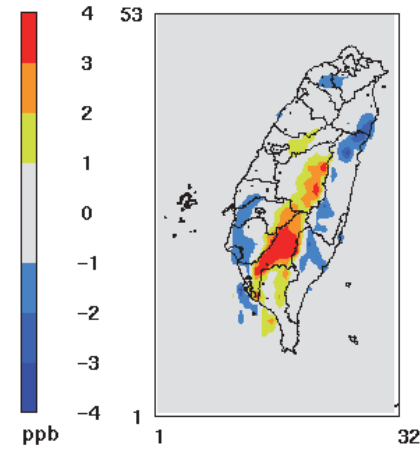


Fig. 6 Spatial Distribution of Difference of Maximum Ozone Hourly Concentration at 14:00, May 25, 2003: Simulation Result Differences before and after Updating Land Use Database.

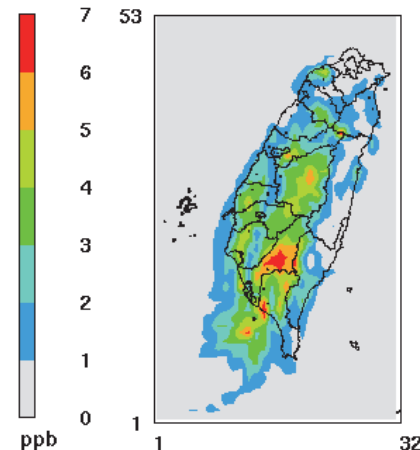


Fig. 7 Spatial Distribution of Greatest Difference of Daily Maximum Ozone Hourly Concentration during the period of May 21-30, 2003: Simulation Result Differences before and after Updating Land Use Database.

3.4 Performance of Air Quality Modeling Results

Quantitative analysis is usually required for evaluating simulation results to determine the differences between simulations and observations, including maximum concentration bias (MB), overall bias (OB) and gross error (GE). Allowances of these three values are specified; MB in ozone should be within $\pm 10\%$, OB within $\pm 15\%$ and GE within 35%, according to the guideline for air quality modeling performance evaluation reg-

ulated by the Environmental Protection Administration of Taiwan. In particular, the OB of the average concentration of the same simulated and observed hourly O₃ data were calculated to verify the extent of under- or over-estimation in the model. The O₃ observations of less than 30 ppb were rejected prior to calculations of OB and GE. The equations are expressed as follows:

$$MB = \frac{1}{N_d} \sum_{j=1}^N \left(\frac{\text{Max}_{i=1}^{24}(P_{i,j}) - \text{Max}_{i=1}^{24}(O_{i,j})}{\text{Max}_{i=1}^{24}(O_{i,j})} \right)$$

$$OB = \frac{1}{N_h} \sum_{i=1}^N \left(\frac{P_i - O_i}{O_i} \right)$$

$$GE = \frac{1}{N_h} \sum_{i=1}^N \left| \frac{P_i - O_i}{O_i} \right|$$

in which, *Max* = the maximum value among all the indicated data; *P_{i,j}* = the estimated concentration at the *i* hour of the *j* day (weather station); *O_{i,j}* = the observed concentration at the *i* hour

of the *j* day (weather station); *N_d* = number of simulation days; *P_i* = the simulated concentration at the *i* hour(weather station); *O_i* = the observed concentration at the *i* hour (weather station); and *N_h* = number of simulation hours.

Air quality simulations for two different BVOC emissions were conducted and a quantitative analysis of ozone concentration was also made. The performance evaluation of the ozone simulation results before and after updating land use database during the period of May 21-30, 2003 is shown in Table 3. The simulation results of ozone concentrations after updating the land use database improve MB, OB and GE significantly for almost every parts of Taiwan. The bias of daily maximum ozone hourly concentration (MB) can be reduced to 9.3% from 11.6% for northern Taiwan, while that is reduced to 0.6% from 2.0% for central Taiwan. The benchmark of performance indicators conventionally used for excellent O₃ simulation are ±10% for MB, ±15% for OB and 35% for GE (GEPD 2009; Boylan and Russell 2006). All indicators are met for the four parts of Taiwan, except of MB in eastern Taiwan and GE in southern Taiwan, but both of them have been improved. This shows that updating the biogenic land use database renders excellent effect of improving air quality modeling.

Table 3 Comparison of Performance Evaluation of Ozone Simulation Results before and after Updating Land Use Database during the Period May 21-30, 2003

| Regions | Maximum Bias (MB) | | Overall Bias (OB) | | Gross Error (GE) | |
|-----------------|-------------------------|--------------------------|-------------------------|--------------------------|-------------------------|--------------------------|
| | After updating land use | before updating land use | After updating land use | before updating land use | After updating land use | before updating land use |
| Northern Taiwan | 9.3 | 11.6 | -1.5 | 2.0 | 31.0 | 31.9 |
| Central Taiwan | 0.6 | 2.0 | -3.2 | -4.1 | 30.2 | 30.5 |
| Southern Taiwan | -4.7 | -5.4 | -4.2 | -4.9 | 36.0 | 38.4 |
| Eastern Taiwan | 12.4 | 13.9 | 3.7 | 4.6 | 20.0 | 20.2 |

4. CONCLUSIONS

As there had been no update to the land use database available in Taiwan for the past decade, satellite remote sensing data was applied to update the existing land use database in this study. In this way, the inventory of biogenic emissions could be conducted more realistically and simulation results of air quality modeling would be more accurate.

Biogenic emissions obtained by the use of TBEIS-2, combined with the new land use database were utilized to simulate air quality by the TAQM. The result indicates ozone concentration in some areas of Taiwan increased. Quantitative analysis shows the results of air quality modeling were close to observed data. It is known thus that updating the land use database renders excellent effect of improving air quality modeling.

REFERENCES

- Basnyat, P., Teeter, L.D., Lockaby, B.G., and Flynn, K.M. (2000). "The use of remote sensing and GIS in watershed level analyses of non-point source pollution problems." *Forest Ecol. Manag.*, **128**, 65-73.
- Boylan, J.W. and Russell, A.G. (2006). "PM and Light Extinction Model Performance Metrics, Goals, and Criteria for Three-Dimensional Air Quality Models." *Atmos. Environ.*, **40**, 4946-4959.
- Chang, C.T. (1999). "South Taiwan Air-Quality Management Plan-Subproject A4: Integration and Estimation of the Agriculture, Forestry, Mining Industry, and Sundries Emissions." EPA-88-FA21- 03-0012; Taiwan EPA, Taipei. (in Chinese)
- Chang, J.S. (principal author), (1990). "The regional acid deposition model and engineering model." Acidic Deposition: State of Science and Technology Report 4, National Acid Precipitation and Assessment Program, Washington, DC. 130pp.

- Chang, J.S., Brost, R.A., Isaksen, I.S.A., Madronich, S., Middleton, P., Stockwell, W.R., and Walcek, C.J. (1987). "A three-dimensional Eulerian acid deposition model, physical concepts and formulation." *J. Geophys. Res.*, **92**, 14681-14700.
- Chang, K.H. (2008). "Modeling approach for emission reduction of O₃ precursors in southern Taiwan." *Atmos. Environ.*, **42**, 6733-6742.
- Chang, K.H., Chen, T.F., and Huang, H.C. (2005). "Estimation of Biogenic Volatile Organic Compounds Emissions in Subtropical Island – Taiwan." *Sci. of the Total Environ.*, **346**, 184-199.
- Chang, K.H., Jeng, F.T. Tsai, T.L., and Lin, P.L. (2000). "Modeling of long-range transport on Taiwan's acid deposition under different weather conditions." *Atmos. Environ.*, **34**, 3281-3295.
- Chang, K.H., Yu, J.H., Chen, T.F., and Lin, Y.P. (2009). "Estimating Taiwan biogenic VOC emission: leaf energy balance consideration." *Atmos. Environ.*, **43**, 5092-5100.
- Chen, G., Li, S., Knibbs, L.D., Hamm, N.A.S., Cao, W., Li, T., Guo, J., Ren, H., Abramson, M.J., and Guo, Y. (2018). "A machine learning method to estimate PM2.5 concentrations across China with remote sensing, meteorological and land use information." *Sci Total Environ.*, **636**, 52-60.
- Chen, T.F. and Chang, K.H. (2006). "Formulating the relationship between ozone pollution features and the transition value of photochemical indicators." *Atmos. Environ.*, **40**, 1816-1827.
- Chen, T.F., Chang, K.H., and Tsai, C.Y. (2019). "A modeling study of assessment of the effectiveness of combining foreign and local emission control strategies." *Atmos. Research*, **224**:114-126.
- Chen, X.L., Zhao, H.M., Li, P.X., and Yin, Z.Y. (2006). "Remote sensing image-based analysis of the relationship between urban heat island and land use/cover changes." *Remote Sens. Environ.*, **104**, 133-146.
- Cheng, G., Han, J., Guo, L., Liu, Z., Bu, S., and Ren, J. (2015). "Effective and Efficient Midlevel Visual Elements-Oriented Land-Use Classification Using VHR Remote Sensing Images." *IEEE Transactions on Geos. and Remote Sens.*, **53**, 8:4238-4249.
- CTCI (1999). "Total Mass Control System for Air Pollutants and the Establishment of Standard Methods for Air Pollutants Emission Inventory." Taiwan EPA, Taipei. (in Chinese).
- Feldman, M.S., Howard, T., McDonald-Buller, E., Mullins, G., Allen, D.T., Webb, A., and Kimura, Y. (2007). "Applications of satellite remote sensing data for estimating dry deposition in eastern Texas." *Atmos. Environ.*, **41**, 7562-7576.
- GEPD (2009). "Proposed Georgia's State Implementation Plan for the Nonattainment Area for Catoosa and Walker Counties." Georgia Department of Natural Resources, Environmental Protection Division.
- Grell, G.A., Dudhia, J., and Stauffer, D.R. (1993). "A Description of the Fifthgeneration Penn State/NCAR Mesoscale Model (MM5)." NCAR/TN-398+STR. NCAR Technical Note, Boulder, CO, 117 pp.
- Guenther, A., Zimmerman, P., Harley, P., Monson, R., and Fall, R. (1993). "Isoprene and monoterpene emission rate variability: model evaluations and sensitivity analyses." *J. Geophys. Res.*, **98**, 12609-12617.
- Guenther, A., Hewitt, C.N., Erickson, D., Fall, R., Geron, C., Graedel, T., Harley, P., Klinger, L., Lerdau, M., McKay, W.A., Pierce, T., Scholes, B., Steinbrecher, R., Tallamraju, R., Taylor, J., and Zimmerman, P. (1995). *J. Geophys. Res.*, **100**, 8873-8892.
- Kheir, R.B., Abdallah, C., Runnstrom, M., and Martensson, U. (2008). "Designing erosion management plans in Lebanon using remote sensing, GIS and decision-tree modeling." *Landscape and Urban Planning*, **88**, 54-63.
- Liu, S.H., Ting, W.H.J., Hsieh, Y.C., and Lin, C.W. (2019). Enhancement of toluene degradation and electricity generation using spirulina microalgae in a microbial fuel cell." *J. of Innovative Technology*, **1**, 1:29-36.
- Ohara, T., Akimoto, H., Kurokawa, J., Horii, N., Yamaji, K., Yan, X., and Hayasaka, T. (2007). "An Asian emission inventory of anthropogenic emission sources for the period 1980-2020." *Atmos. Chem. Phys. Discuss.*, **7**, 6843-6902.
- Pandey, V.K., Panda, S.N., Pandey, A., and Sudhakar, S. (2009). "Evaluation of effective management plan for an agricultural watershed using AVSWAT model, remote sensing and GIS." *Environ. Geology*, **56**, 993-1008.
- Peng, J., Wu, J., Yin, H., Li, Z., Chang, Q., and Mu, T. (2008). "Rural land use change during 1986-2002 in Lijiang, China, based on remote sensing and GIS data." *Sensors*, **8**, 8201-8223.
- Stockwell, W.R., Middleton, P., and Chang, J.S. (1990). "The second generation regional acid deposition model chemical mechanism for regional air quality modeling." *J. Geophys. Res.*, D10, **95**, 16343-16367.
- Streets, D.G., Bond, T.C., Carmichael, G.R., Fernandes, S.D., Fu, Q., He, D., Klimont, Z., Nelson, S.M., Tsai, N.Y., Wang, M.Q., Woo, J.H., and Yarber, K.F. (2003). "An inventory of gaseous and primary aerosol emissions in Asia in the year 2000." *J. Geophys. Res.*, **108**, 8809, doi:10.1029/2002JD003093.
- Wang Z.H., Bai, Y.H., and Zhang, S.Y. (2003). "A biogenic volatile organic compounds emission inventory for Beijing." *Atmos. Environ.*, **37**, 3771-3782.
- Wiedinmyer, C., Guenther, A., Estes, M., Strange, I.W., Yarwood, G., and Allen, D.T. (2001). "A land use database and examples of biogenic isoprene emission estimates for the state of Texas." USA, *Atmos. Environ.*, 6465-6477.